

# Improvement of high-temperature mechanical properties of heat treated $C_f$ /geopolymer composites by Sol- $SiO_2$ impregnation

Peigang He, Dechang Jia<sup>\*</sup>, Meirong Wang, Yu Zhou

*Institute for Advanced Ceramics, Harbin Institute of Technology, No. 2 Yikuang Street, Harbin 150080, PR China*

Received 30 March 2010; received in revised form 1 July 2010; accepted 19 July 2010

Available online 14 August 2010

## Abstract

Unidirectional carbon fiber reinforced geopolymer composite was prepared by ultrasonic-assisted slurry infiltration method and heat treated at 1100 °C. Then it was impregnated with Sol- $SiO_2$  to seal the cracks and pores formed during heat treatment. The ambient strength of composite after impregnation was enhanced by 35.6% due to the increase relative density from the starting 79% to 93.6%. Composites both before and after impregnation fractured in a non-brittle manner at both ambient and high temperatures. Over an elevated temperature range from 700 to 900 °C, the strength of the two composites showed anomalous gains and reached their maximum values at 900 °C, 322.1 and 425.1 MPa, respectively. These values were 19.8% and 16.8% higher than their ambient ones. When the temperature was further increased to 1100 °C, the impregnated composite showed superior high-temperature properties, which was attributed to the improved fiber integrity due to the Sol- $SiO_2$  sealing effect. Crown Copyright © 2010 Published by Elsevier Ltd. All rights reserved.

**Keywords:** Composite; Relative density; High-temperature mechanical strength; Fracture behavior

## 1. Introduction

Geopolymer is a kind of inorganic polymer material with low density, low cost, easy processing, environmentally friendly nature and excellent thermal properties.<sup>1–5</sup> Compared with polymer, geopolymer materials can be used under much more higher temperature such as above 1000 °C and they tend to be uncombustible and no poisonous smoke would be released.<sup>6</sup> Therefore, geopolymer materials have recently shown significant promise as aircraft cabin and heat resistant materials, and have been investigated as an alternative to polymer composites.<sup>6,7</sup> However, pure geopolymer matrix exhibits relatively low mechanical properties, which is a great impediment to their wide applications.

Over the past years, some studies have been carried out on geopolymer matrix composites reinforced by particulate,<sup>3,4</sup> continuous fiber<sup>5–9</sup> and short fiber,<sup>10,11</sup> etc., and many impressive results have been achieved. Among them, continuous fiber reinforced geopolymer composites have received a lot of attention for their adaptability to conventional techniques in polymer com-

posites manufacturing. Meanwhile, due to their high strength and modulus, the fibers can prevent catastrophic brittle failure in composites.

Recently, some researchers have concentrated their attention on the high-temperature behavior of the geopolymer and geopolymer composites. Provis et al.<sup>12</sup> identified the correlation between mechanical properties and thermal dilatometric performance, and reported that geopolymer which showed a small expansion after heat treatment displayed the best strength. Geopolymer made with fly ash exhibited strength increases after 800 °C exposure, whilst geopolymer/aggregate composite decreased in strength after the same exposure due to the great thermal incompatibility<sup>13</sup>; the addition of  $\alpha-Al_2O_3$  particles increased the strength of geopolymer composites, and after exposure at temperature between 800 and 1200 °C, both geopolymer and composites got significant gain in strength due to the viscous sintering.<sup>14</sup> Reis et al.<sup>15</sup> recently reported that though both the strength and stiffness of carbon or glass fibers reinforced HIGH-SILICA geopolymer composites decreased with increasing temperature from room temperature until 300 °C, the major drop on both the stiffness and strength did not occur until 150 °C. The literature suggested that the effect of high temperature on the properties of geopolymer materials depended on the aluminosilicate source, alkali cation, Si/Al

<sup>\*</sup> Corresponding author. Tel.: +86 451 86418792; fax: +86 451 86414291.  
E-mail address: [dcjia@hit.edu.cn](mailto:dcjia@hit.edu.cn) (D. Jia).

ratio, and thermal compatibility between matrix and reinforcements.

In our recent research<sup>16</sup> we reported that continuous carbon fiber reinforced geopolymer composite exhibited good mechanical properties, and proper high-temperature heat treatment was an efficient way to further improve its mechanical properties. However, many cracks and pores appeared in the composite after heat treatment. These defects would be unfavorable to the high-temperature mechanical properties of composites in air because of carbon fiber degradation. Repeated impregnation of slurry with low viscosity into the composites is an efficient method to seal these defects and to further improve the mechanical properties of the composite. This has been widely used in fabrication of composites by polymer infiltration and pyrolysis (PIP) process.<sup>17–19</sup>

Therefore, in this paper Sol-SiO<sub>2</sub> was used for impregnation considering its low price, low viscosity, high solid content and excellent thermal properties. The impregnation routes of Sol-SiO<sub>2</sub> into composites were optimized. The room and high-temperature mechanical properties of composite both before and after impregnation were systematically investigated. Relevant studies were rarely reported before.

## 2. Experimental procedures

Geopolymer resin with composition of SiO<sub>2</sub>/Al<sub>2</sub>O<sub>3</sub> = 5, K<sub>2</sub>O/SiO<sub>2</sub> = 0.2 and H<sub>2</sub>O/K<sub>2</sub>O = 11 (mole ratio) was obtained by mixing metakaolin powder with potassium silicate solution. The metakaolin was prepared by calcining kaolin at 800 °C for 3 h. The main phase of metakaolin was amorphous with minor

α-quartz.<sup>16</sup> The potassium silicate solution was prepared by dissolving amorphous silica (Shanghai Dixiang Indus, China) into KOH (Tianjin Fuchen Indus., China) solution. The solution was then allowed to mature under stirring for 48 h in order to dissolve the silica completely.<sup>20</sup>

The carbon fiber used in this study (Jilin Carbon Indus., China) has a diameter of 6–8 μm, and an average tensile strength of 2800 MPa. The composite was prepared by infiltrating geopolymer resin into the unidirectional continuous PAN-based carbon fiber perform. The preparation process of the composite was described in our previous study.<sup>16</sup> After that, the composite sample was heat treated at 1100 °C for 90 min in an argon atmosphere. The as-achieved composite was machined and polished into specimens with a dimension of 3.0 mm × 4.0 mm × 30.0 mm. The apparent porosity was ca. 20% measured by the Archimedes method.

The specimens were divided into 4 groups, 3 of which were further impregnated by Sol-SiO<sub>2</sub> of 20, 30, and 40 wt.% concentrations under vacuum for 8 h. After drying at 200 °C for 2 h, excess slurry was removed from the surface of the performs and specimens were repeatedly impregnated. The vacuum impregnation and drying process was repeated 6 times. At last the impregnated specimens were heat treated at 900 °C.

Flexural strength measurements of composites were conducted on specimens (4 mm × 3 mm × 36 mm) using a three-point-bending fixture on an Instron-500 tester with a span length of 30 mm at a crosshead speed of 0.5 mm/min. Specimens were machined with the tensile surface perpendicular to the direction of lamination. Load–displacement curves were recorded. Work of fracture was calculated by the area between

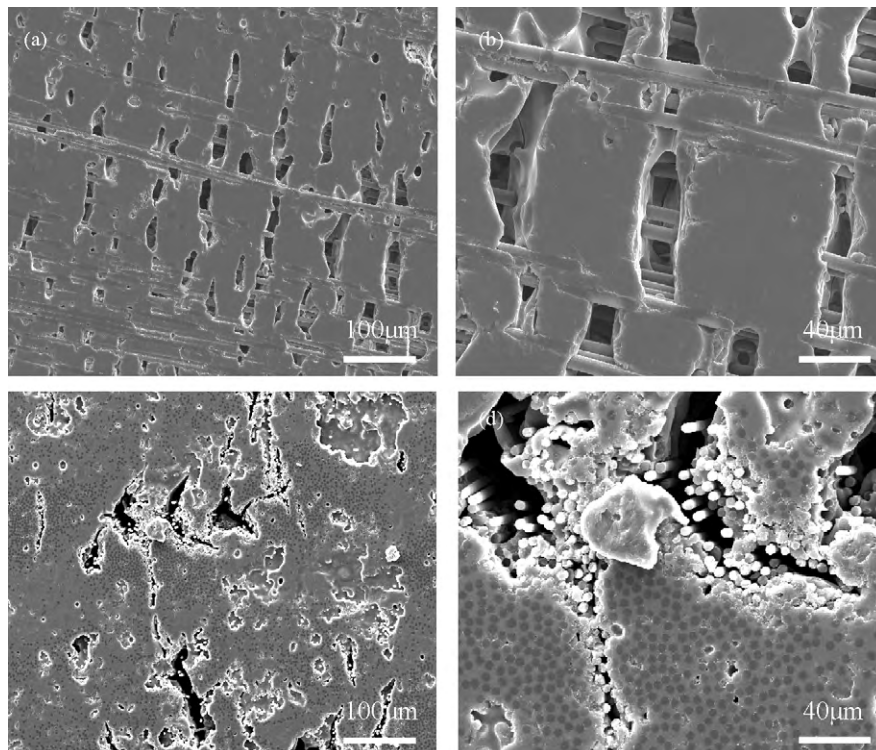


Fig. 1. Microstructure of the polished cross-section of composite before impregnation: in the axial direction of fibers (a) and (b); and in the radial direction (c) and (d).

the load curve and  $X$  axis in the load/displacement curves till the load drops to 90% of the maximum. Six specimens were tested under each test condition and average values were finally reported. The tested temperatures were room temperature, 700, 900 and 1100 °C in air. Composites before and after Sol-SiO<sub>2</sub> impregnation were denoted as HC and ImHC, respectively. And the high-temperature tested samples were denoted as (Im)HC-R, (Im)HC-700, (Im)HC-900 and (Im)HC-1100, respectively. Microstructure of the polished surface and fractograph of the composites were observed by scanning electron microscopy (SEM, FEI, Quanta-200).

### 3. Results and discussion

As shown in Fig. 1, after heat treatment many cracks and pores were formed in HC specimens, leading to the carbon fibers partially naked to the air. According to the carbon fiber oxidation kinetics analyses,<sup>21</sup> carbon fibers were susceptible to oxidation, thus it was necessary to seal these cracks and pores. In our investigation, Sol-SiO<sub>2</sub> was used to seal the defects and to enhance the resistance of composite to oxidation in high temperature.

#### 3.1. Optimization of Sol-SiO<sub>2</sub> impregnation

The effect of Sol-SiO<sub>2</sub> concentration on the relative density (RD) of composites is shown in Fig. 2. When Sol-SiO<sub>2</sub> concentration was increased from 20 to 40 wt.%, an increased RD was observed after the first impregnation cycle. However, after the subsequent cycles RD increased more slowly to Sol-SiO<sub>2</sub> concentration of 40 wt.% than those of 20 and 30 wt.%, which

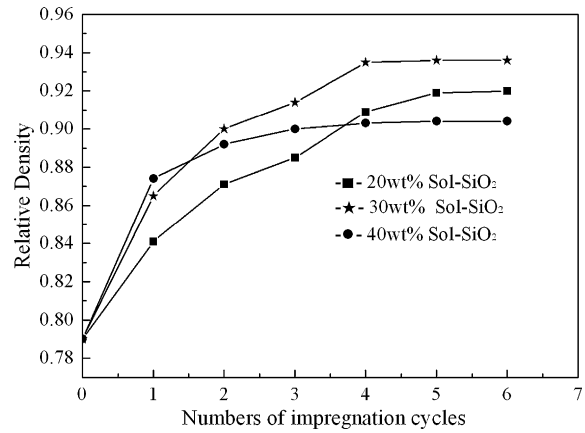


Fig. 2. Relative density vs. number of impregnation/drying cycles with different Sol-SiO<sub>2</sub> concentrations.

may be ascribed to the formation of more closed pores hampering any further Sol-SiO<sub>2</sub> infiltration process. After 4 times of impregnation cycles, the highest relative density (93.6%) could be obtained for 30 wt.% Sol-SiO<sub>2</sub>. Thus 30 wt.% Sol-SiO<sub>2</sub> was selected as the impregnation solution.

Fig. 3 shows the microstructure of composites impregnated with 30 wt.% Sol-SiO<sub>2</sub> for 6 times and treated at 800 °C. It can be seen that most pores were filled and cracks healed by the SiO<sub>2</sub> particles, as identified by EDS elemental analyses (Fig. 4). Fig. 3(a) shows that except for the surface fibers, few internal fibers in ImHC were naked to the air, as compared with those in HC specimens. This was beneficial for improving the oxidation resistance of the composite. However, in the magnified microstructure in the insert picture of Fig. 3(b), microcracks

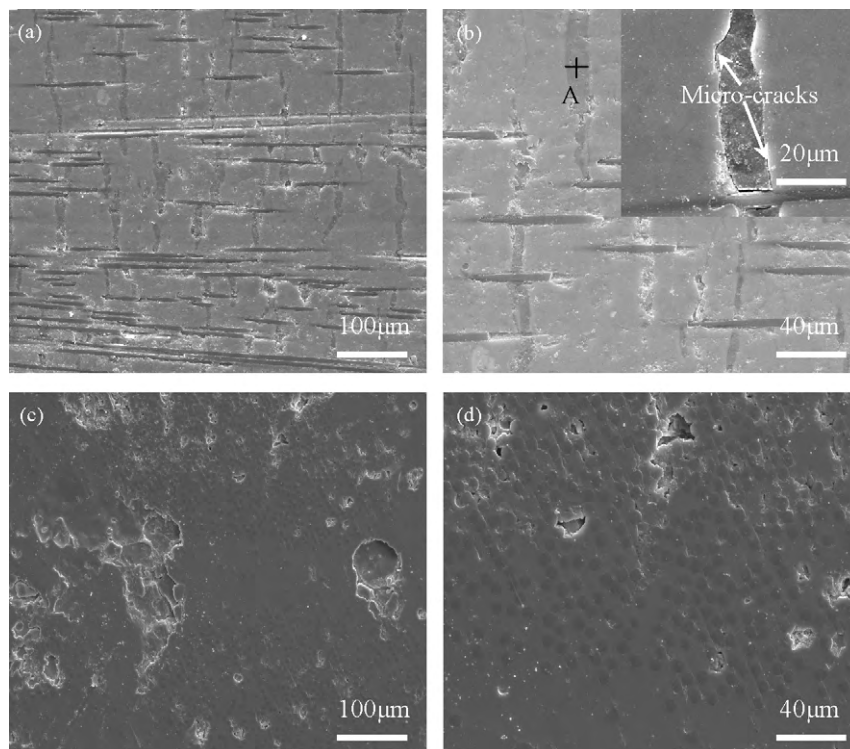


Fig. 3. Microstructure of the polished cross-section of composite after impregnation: in the axial direction of fibers (a) and (b); and in the radial direction (c) and (d).

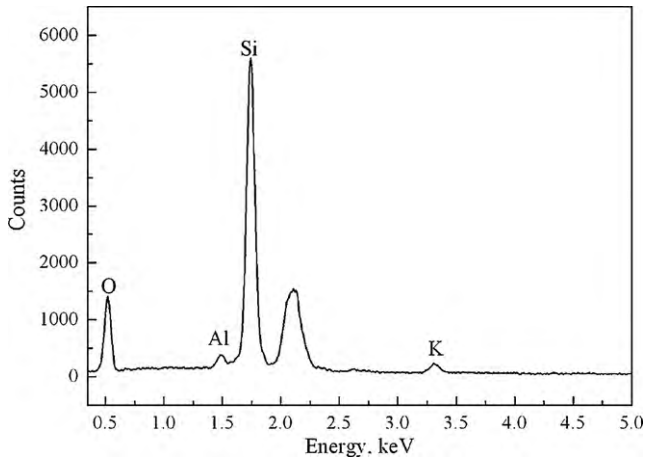


Fig. 4. Energy dispersive spectrum of point A in Fig. 3(b).

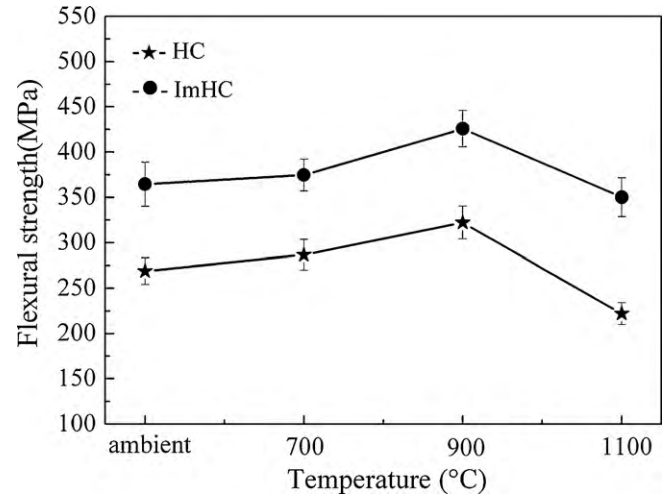


Fig. 5. Flexural strength vs. temperature of the two composites.

Table 1  
Elevated temperature flexural strength and work of fracture of HC and ImHC samples.

Specimen	Density (g/cm <sup>3</sup> )	Relative density (%)	T (°C)	Mechanical properties	
				Flexural strength (MPa)	Work of fracture (J m <sup>-2</sup> )
HC	1.81	79.0	RT	268.9 ± 14.6	5003.4 ± 254.4
			700	286.6 ± 16.8 (6.6%)	5127.9 ± 314.3
			900	322.1 ± 18.2 (19.8%)	5796.2 ± 241.4
			1100	221.9 ± 12.2 (-17.5%)	4072.1 ± 307.9
ImHC	2.16	93.4	RT	364.7 ± 24.4	6527.4 ± 342.1
			700	374.7 ± 17.6 (2.9%)	6794.7 ± 269.2
			900	425.8 ± 20.1 (16.8%)	7408.3 ± 275.8
			1100	350.1 ± 21.3 (-4.0%)	6009.5 ± 259.7

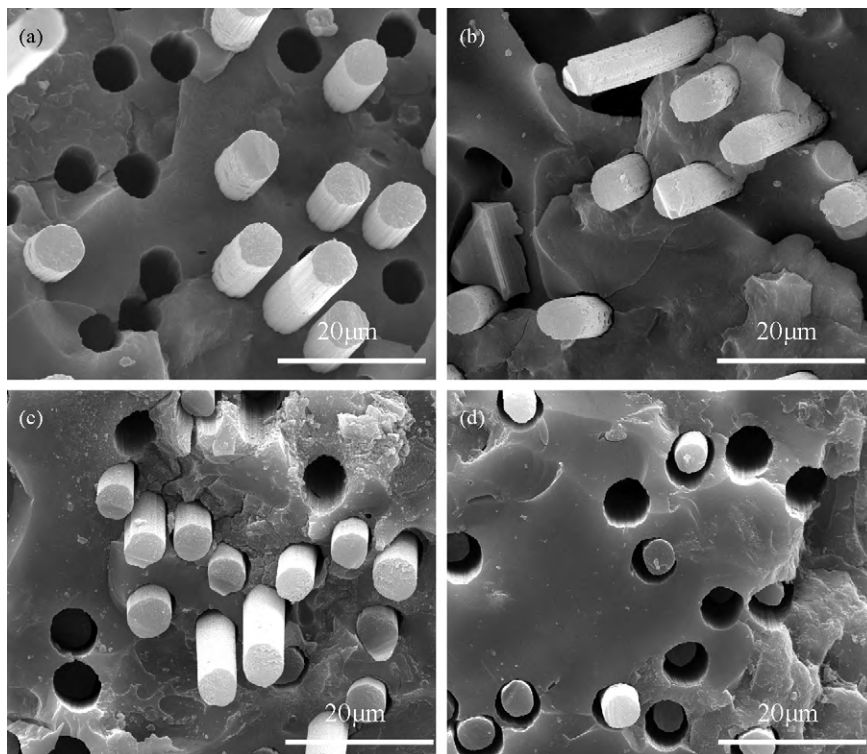


Fig. 6. SEM observations of ImHC after flexural strength test at (a) RT, (b) 700 °C, (c) 900 °C, and (d) 1100 °C. Samples were prepared by broking-off the ImHC specimens in cryogenic liquid nitrogen and the similar positions were selected for observation in each sample.

could also be observed which might be due to the thermal mismatch between leucite matrix and SiO<sub>2</sub> particles. In Fig. 3(d), a few dispersed residual pores still could be observed in the intra-bundle regions. During the impregnation process, the size and number of residual pores left in the inter- and intra-bundle areas gradually decreased. When the residual pores were small enough, the viscous Sol-SiO<sub>2</sub> solution could not be effectively infiltrated into the composite thus these small pores were left in the composites, which had been well studied in composites prepared by precursor impregnation and pyrolysis.<sup>22</sup>

### 3.2. Room and elevated temperature mechanical property

Fig. 5 shows the curves of two composites flexural strength vs. the testing temperature, and Table 1 summarizes the elevated temperature strength values and their increase rate compared with room temperature strength value. After impregnation, the flexural strength increased by about 35%, as compared with that before impregnation. At 700 °C, the flexural strength of the two composites increased slightly. At 900 °C, the bending strength grew rapidly and reached their maximum value, 322.1 and 425.8 MPa, which were 19.8% and 16.8% higher than their room temperature strength values, respectively. As temperature further increased, the bending strength slightly decreased, but even at 1100 °C, they still could retain very high values, 221.9 and 350.1 MPa, which were 82.5% and 96.0% of their respective room temperature strength. The work of fracture of the composites showed a similar trend as the flexural strength. The high-temperature mechanical strength of both composites in our study was much higher than those in previous research.<sup>3</sup> David reported that at 1000 °C carbon fiber and glass fiber reinforced geopolymer composites lost most of their strength, and composite reinforced by SiC fibers only retained about 66% of the room temperature strength.

The initial target of this investigation was to lower the strength loss rate of the composites at high temperature by Sol-SiO<sub>2</sub> impregnation. However, at 700 and 900 °C anomalous strength gain for both composites were observed, such that the maximum strength was increased by as high as 19.8%. The anomalous strength gain of composites at certain temperature range might be a result from the relaxation of residual stress. In the case of the composite obtained in our study, the coefficient of thermal expansion (CTE) of matrix ( $15.4 \times 10^{-6} \text{ K}^{-1}$ ) was much higher than that of carbon fiber ( $1 \times 10^{-6} \text{ K}^{-1}$ ). Then, the tensile residual stress on the matrix and the compressive residual stress on fibers would have taken place. At high temperature, the residual stress was released, leading to matrix cracks closing and efficient load transferring from matrix to fiber. Meanwhile, at lower temperature the inner carbon fibers of the composites were protected from being oxidized by the cracks-terminated matrix and most fibers maintained fine integrity (Fig. 6(b) and (c)) similar to that of ImHC-RT specimen (Fig. 6(a)). Consequently, composite showed an increased strength over this temperature range. However, when the temperature was further increased to 1100 °C, though relaxation of residual stress still occurred, fiber degradation (as shown in Fig. 6(d), which is discussed in the later part) played a negative role, leading to the strength decrease. Simi-

lar trends were also observed in SiC<sub>f</sub>/SiC–Al<sub>2</sub>O<sub>3</sub>–Y<sub>2</sub>O<sub>3</sub>–CaO<sup>23</sup> and C<sub>f</sub>/SiO<sub>2</sub>–Si<sub>3</sub>N<sub>4</sub> composites.<sup>24</sup> From the strength retaining rate values shown in Table 1, it can be implied that the composite after impregnation showed better fiber oxidation resistance than the other at 1100 °C. This was due to the Sol-SiO<sub>2</sub> sealing effect based on satisfying impregnation which was more beneficial to protect carbon fiber from being oxidized. Therefore, the geopolymer technology, together with Sol-SiO<sub>2</sub> impregnation, might provide a new method of low-cost and short-time fabrication of the C<sub>f</sub>/ceramic composite, which exhibited good high-temperature mechanical properties and might be attractive for application at elevated temperature.

Furthermore, Fig. 7 shows the typical stress–displacement curves of the composites at room and elevated temperatures, indicating the effect of testing temperature. All the composites showed non-catastrophic fracture behavior. After the initial elastic region, the non-linear region appeared which could be caused by fiber-bridging and sliding after debonding. After reaching the maximum strength there was several significant steep drop-steps and developed a long tails, which was resulted from fiber breakage and pull-out. For all specimens tested, the fibers submitted to compressive stresses did not break and the main failure process occurred in tension side as shown in Fig. 8, indicating

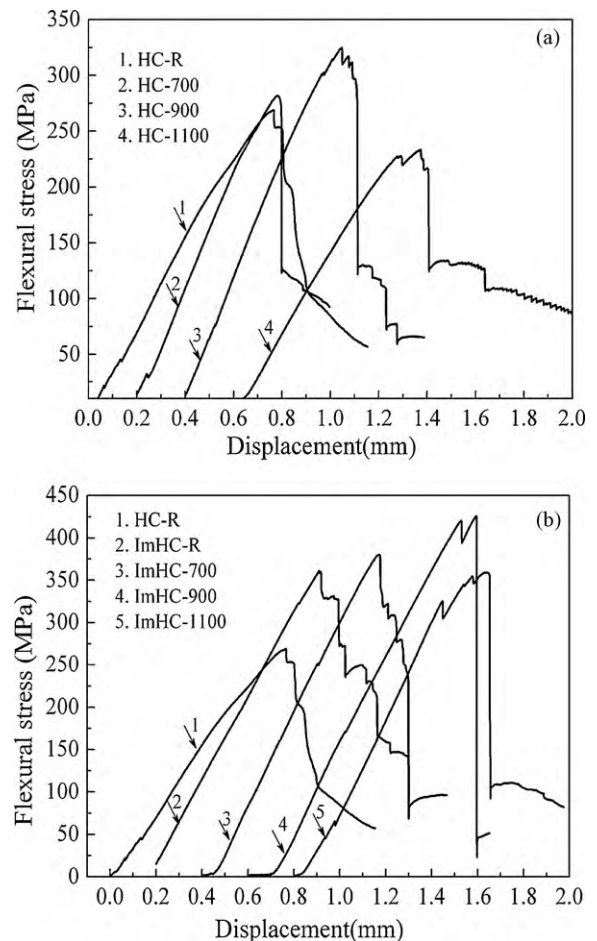


Fig. 7. Typical load–displacement curves corresponding to their flexural strength tests at different temperatures: (a) HC and (b) ImHC.

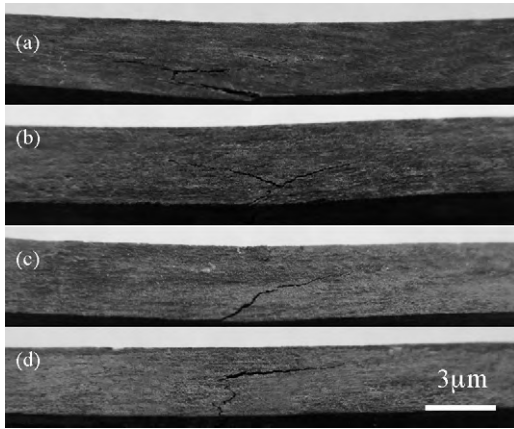


Fig. 8. Typical morphologies of ImHC specimens after flexural tests at (a) RT, (b) 700 °C, (c) 900 °C, and (d) 1100 °C.

that all specimens fractured in tensile fracture mode. Studies developed by Reis et al.<sup>15</sup> showed that carbon or glass fibers reinforced HIGH-SILICA geopolymer composites fractured in a different mechanism, i.e. the compressive fracture mode. They reported that the high compressive stress concentration in the pin load contact region associated with the low compressive strength of the fibers, promoted compressive breakage of the longitudinal fibers in this region. Such different fracture mechanisms of these composites might be attributed to the different properties of matrix and their specific microstructures.<sup>25</sup> The matrix of the composites in our investigation was leucite ceramic which possessed much higher strength and stiffness than the geopolymer, and the  $C_f$ /matrix interface bonding was just in a good

state.<sup>16</sup> Meanwhile, the fiber volume fraction in our investigation was much lower than those investigated by Reis et al. (25% vs. 55%). The stronger matrix and the desirable  $C_f$ /matrix interface, together with the lower fiber volume fraction, would be beneficial to the load transfer from matrix to the carbon fiber efficiently through the interface, and eventually resulted in the tensile fracture mode of the composite.

After impregnation, composite displayed not only higher room temperature failure stress but also higher elastic modulus, as observed from the initial linear stage of the curves. The increased mechanical properties were attributed to the increased relative density, which facilitated the load transfer from the matrix to the fiber.<sup>14</sup> No evident plastic deformation exhibited from all the stress–displacement curves, implying that the viscous flow of matrix did not occur even at 1100 °C.<sup>20</sup>

Fig. 9 shows the fractographs of composite after impregnation at room and elevated temperatures. All samples exhibited a rough fracture surface with many pulled-out fibers and holes resulted from the pulled-out fibers, indicating the great reinforcement of carbon fiber. The fractographs show that for ImHC-700 and ImHC-900 most fibers maintained fine integrity as well as for ImHC-R, implying a good oxidation resistance of the composites. Whilst for ImHC-1100, fiber degradation was clearly observed. As shown in Fig. 9(d), fiber diameter became finer which were a result from that the carbon fibers had been seriously oxidized when the sample was kept at the high testing temperature in air. Also it can be observed that with increasing testing temperature from room to 1100 °C, pulling-out length of fibers decreased. This may be caused by the fiber oxidation which makes fiber easily broke at the oxidized part. Similar frac-

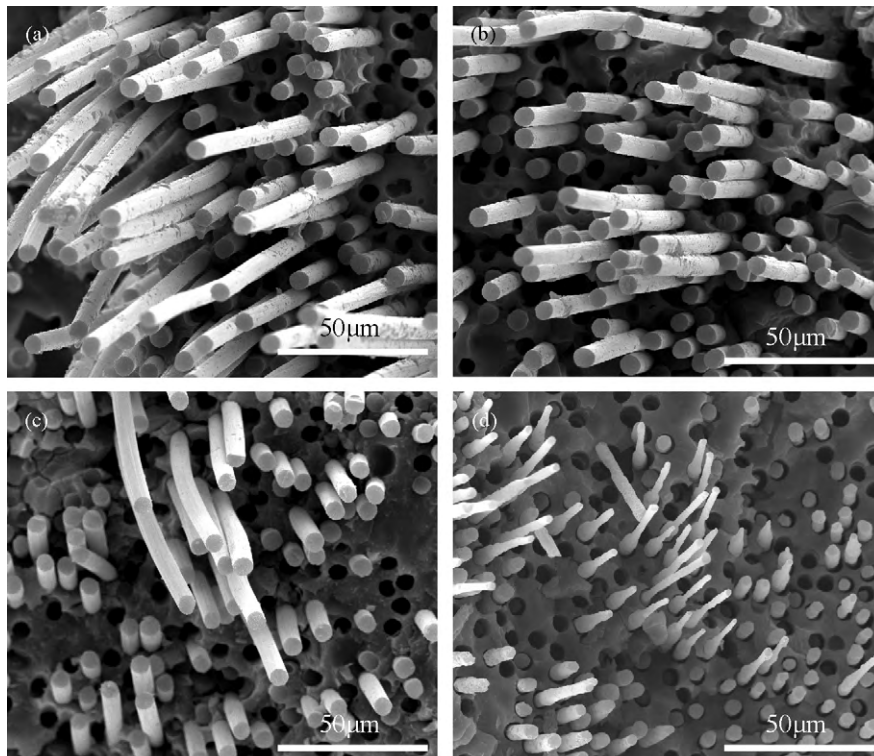


Fig. 9. The morphology of fracture surface near the tensile sides: (a) ImHC-R; (b) ImHC-700; (c) ImHC-900; (d) ImHC-1100.

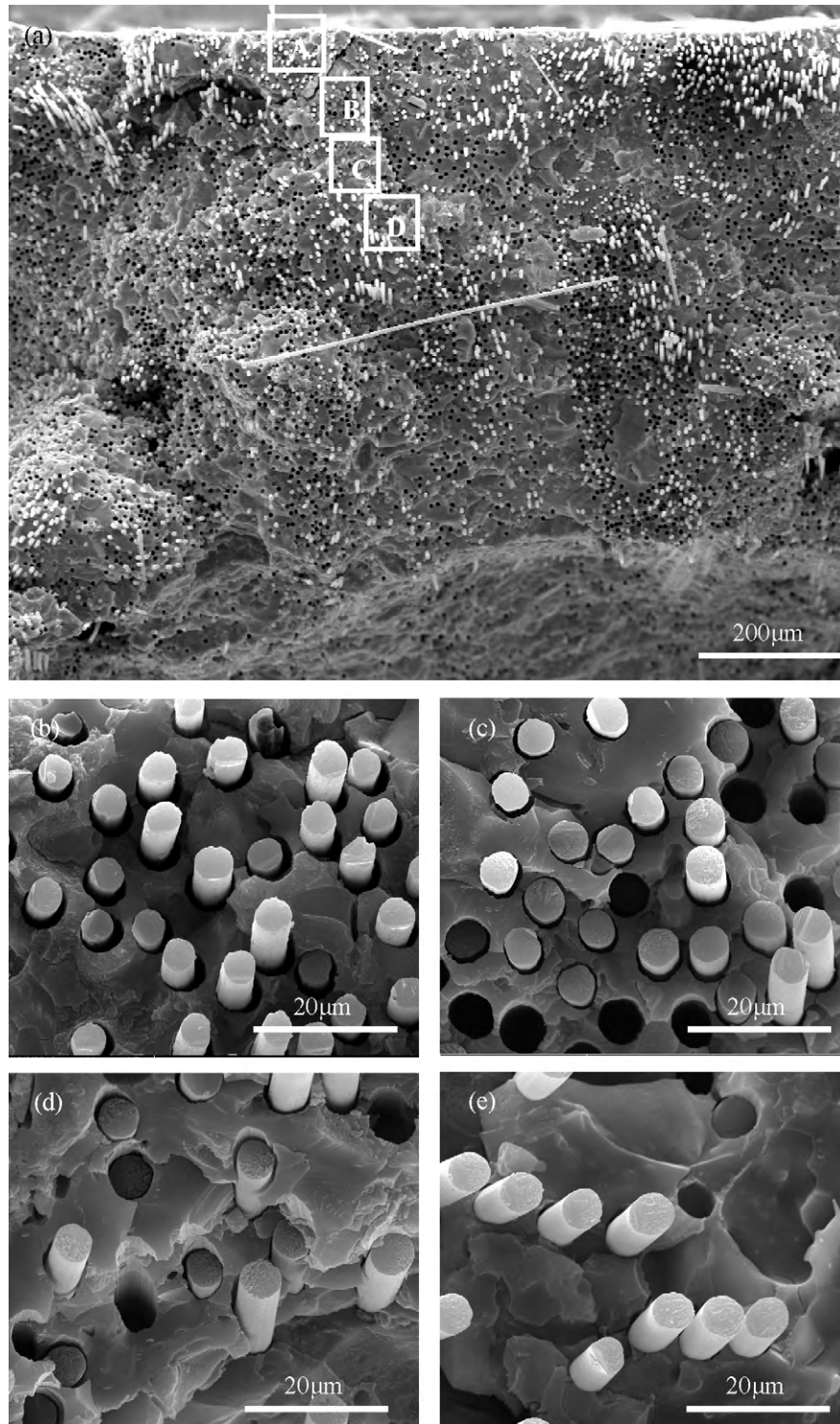


Fig. 10. SEM fractograph obtained at room temperature of ImHC after flexural strength test at 1100: (a) low magnification fractograph, (b)–(e) was corresponding to the area of (A)–(D). Samples were prepared by the same method as mentioned in Fig. 6.

ture morphology of composites before impregnation was also observed, which was not present here.

In order to know the oxidation degree of the carbon fiber at 1100 °C, one ImHC-1100 sample was randomly selected and broken-off for SEM observation. Fig. 10 shows typical fractographs of the composite and indicated that no fiber was

burned out. Fig. 10(b) presents the morphology of the degraded carbon fibers partly oxidized and the increased interstice formed at the  $C_f$ /matrix interface area between carbon fiber and the matrix. With increasing the distance to the surface, integrity of carbon fiber gradually increase, as shown in Fig. 10(b)–(e). Most carbon fibers beyond 200  $\mu\text{m}$  in depth still maintain their

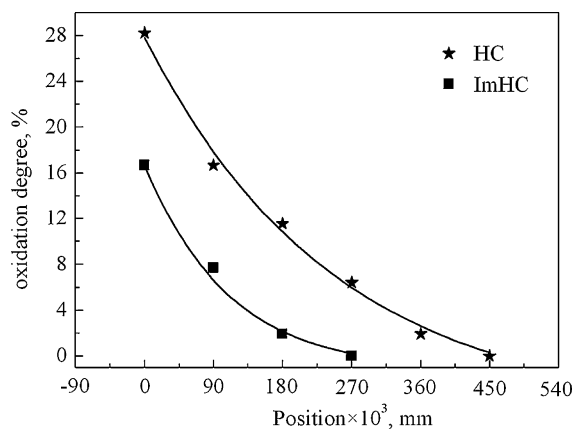


Fig. 11. The degree of fiber oxidation vs. distance from the surface of the two composites.

original morphology, and they were bonded very well with the matrix (Fig. 10(e)).

The degree of fiber oxidation in ImHC-1100 was evaluated as given in formula (1):

$$\text{Degree of oxidation (\%)} = \left(1 - \frac{R_d}{R_0}\right) \times 100 \quad (1)$$

In this equation,  $R_d$  is the average fiber diameter of all carbon fibers in each magnified fractograph from Fig. 10(b)–(e) and each fiber is measured in four directions;  $R_0$  is the original average fiber diameter. The result is shown in Fig. 11 and compared with that in HC-1100 which is calculated using similar method. It was obvious that the oxidation resistance of ImHC at 1100 °C was much better than that of HC as indicated in Fig. 11. The oxidation of carbon fiber in ImHC only took place in the surface layer of about 200 μm in depth, whereas in HC it was about 400 μm in depth. So, it can be suggested from the above that the reinforcement from carbon fibers in ImHC were influenced more slightly than those in HC, which was in good agreement with the elevated temperature strength testing results.

#### 4. Conclusions

This paper reported the effects of Sol-SiO<sub>2</sub> impregnation and testing temperature on the mechanical properties of a heat treated geopolymer matrix composite reinforced with carbon fibers.

- (1) Repeated Sol-SiO<sub>2</sub> impregnation was an efficient method to seal the cracks and pores in the composite and thus greatly enhance the mechanical properties of the composite. The relative density of composite increased from the starting 78% to 93.6% and room temperature strength of composite was enhanced by 35.6% relative to its original state before impregnation.
- (2) Composite both before and after impregnation showed anomalous gain in strength over certain elevated temperature range from 700 to 900 °C. And at 900 °C, the flexural strength of the composites reached the highest values, which were 19.8% and 16% higher than its room temperature strength, respectively. The strength gain behavior

was attributed to the relaxation of residual stress and fiber integrity.

- (3) Compared with un-impregnated composite, the impregnated one showed better fiber oxidation resistance and much higher high-temperature mechanical strength due to its much denser microstructure based on satisfying impregnation. Even at 1100 °C in air, fiber degradation only took place in the surface layer (~200 μm in depth) of the impregnated composite and flexural strength can still retained as high as 96% of the room temperature strength value.

#### Acknowledgements

This work was supported by Program for New Century Excellent Talents in University (NCET, Grant No. NCET-04-0327), Program of Excellent Team in Harbin Institute of Technology and the Science Fund for Distinguished Young Scholars of Heilongjiang Province. We are very grateful to Yi Qin in the Interconnection Group at Loughborough University for his assistance in proofreading.

#### References

1. Davidovits J. Geopolymer—inorganic polymeric new materials. *J Therm Anal* 1991;**37**(8):1633–56.
2. Davidovits J. 30 years of successes and failures in geopolymer applications. In: *Geopolymer Conference*. 2002.
3. Davidovits J, Davidovics M. Geopolymer: ultra-high temperature tooling material for the manufacture of advanced composites. *Sampe* 1991;**36**(2):1939–49.
4. Barbosa VFF, MacKenzie KJD. Thermal behaviour of inorganic geopolymers and composites derived from sodium polysialate. *Mater Res Bull* 2003;**38**(2):319–31.
5. Papakonstantinou CG, Balaguru PN, Lyon RE. Comparative study of high temperature composites. *Compos Part B* 2001;**32**(8):637–49.
6. Lyon RE, Balaguru PN, Foden A, Sorathia U, Davidovits J, Davidovics M. Fire-resistant aluminosilicate composites. *Fire Mater* 1997;**21**(4):67–73.
7. Zhao Q, Nair B, Rahimian T, Balaguru PN. Novel geopolymer based composites with enhanced ductility. *J Mater Sci* 2007;**42**(9):3131–7.
8. Balaguru PN, Defazio C, Arafa MD, Nair B. Functional geopolymer composites for structural ceramic application, Ceram-RU9163, <http://cait.rutgers.edu/files/Ceram-RU9163.pdf>.
9. Nair BG, Zhao Q, Cooper RF. Geopolymer matrices with improved hydrothermal corrosion resistance for high-temperature applications. *J Mater Sci* 2007;**42**(9):3083–91.
10. Zhang YS, Sun W, Li Z, Zhou X. Geopolymer extruded composites with incorporated fly ash and polyvinyl alcohol short fiber. *ACI Mater J* 2009;**106**(1):3–10.
11. Lin TS, Jia DC, He PG, Wang MR, Liang DF. Effects of fiber length on mechanical properties and fracture behavior of short carbon fiber reinforced geopolymer matrix composites. *Mater Sci Eng A: Struct* 2008;**497**(1–2):181–5.
12. Provis JL, Yong CZ, Duxson P, Deventer JSJ. Correlating mechanical and thermal properties of sodium silicate-fly ash geopolymers. *Colloid Surf A* 2009;**336**(1–3):57–63.
13. Daniel LYK, Jay GS. Damage behavior of geopolymer composites exposed to elevated temperatures. *Cement Concrete Compos* 2008;**30**(10):986–91.
14. Lin TS, Jia DC, He PG, Wang MR. Thermo-mechanical and microstructural characterization of geopolymers with α-Al<sub>2</sub>O<sub>3</sub> particle filler. *Int J Thermophys* 2009;**30**:1568–77.
15. Pernica D, Reis PNB, Ferreira JAM, Louda P. Effect of test conditions on the bending strength of a geopolymer-reinforced composite. *J Mater Sci* 2010;**45**:744–9.



16. He PG, Jia DC, Lin TS, Wang MR. Effects of high-temperature heat treatment on the mechanical properties of unidirectional carbon fiber reinforced geopolymer composites. *Ceram Int* 2010;**36**(5):899–905.
17. Lee SH, Weinmann M, Aldinger F. Processing and properties of C/Si–B–C–N fiber-reinforced ceramic matrix composites prepared by precursor impregnation and pyrolysis. *Acta Mater* 2008;**56**(7):1529–38.
18. Dong SM, Katoh Y, Kohyama A, Schwab ST, Snead LL. Microstructural evolution and mechanical performances of SiC/SiC composites by polymer impregnation/microwave pyrolysis (PIMP) process. *Ceram Int* 2002;**28**(8):899–905.
19. Ma QS, Chen ZH, Zheng WW, Hu HF. Effects of pyrolysis processes on microstructure and mechanical properties of C<sub>f</sub>/Si–O–C composites fabricated by preceramic polymer pyrolysis. *Ceram Int* 2005;**31**(2):305–14.
20. Kriven WM, Bell J, Gordon M. Microstructure and microchemistry of fully-reacted geopolymers and geopolymer matrix composites. In: Bansal NP, Singh JP, Kriven WM, Schneider H, editors. *Ceramic transactions, vol. 153, advances in ceramic matrix composites*. Westerville, OH: The American Ceramic Society; 2003. p. 227–50.
21. Halbig MC, McGuffin-Cawley JD, Eckel AJ, Brewer DN. Oxidation kinetics and stress effects for the oxidation of continuous carbon fibers within a microcracked C/SiC ceramic matrix composite. *J Am Ceram Soc* 2008;**91**(2):519–26.
22. Zhu YZ, Huang ZR, Dong SM. Manufacturing 2D carbon-fiber-reinforced SiC matrix composites by slurry infiltration and PIP process. *Ceram Int* 2008;**34**(5):1201–5.
23. Yoshida K, Yano T. Room and high-temperature mechanical and thermal properties of SiC fiber-reinforced SiC composite sintered under pressure. *J Nucl Mater* 2000;**283–287**:560–4.
24. Jia DC, Zhou Y, Lei TC. Ambient and elevated temperature mechanical properties of hot-pressed fused silica matrix composite. *J Eur Ceram Soc* 2003;**23**(5):801–8.
25. Reis PNB, Ferreira JAM, Antunes FV, Costa JDM. Flexural behaviour of hybrid laminated composites. *Compos Part A: Appl Sci Manuf* 2007;**38**:1612–20.